

# Global Significance of a Sub-Moho Boundary Layer (SMBL) Deduced from High-Resolution Seismic Observations

KARL FUCHS,<sup>1</sup>

*Geophysical Institute, University Karlsruhe, Hertz-Str. 16, D-76187 Karlsruhe, Germany*

MARC TITTEMEYER,

*Max-Planck-Institute of Cognitive Neuroscience, Stephanstr. 1, D-04103 Leipzig, Germany*

TROND RYBERG,

*GeoForschungsZentrum, Telegrafenberg, D-14473 Potsdam, Germany*

FRIEDEMANN WENZEL,

*Geophysical Institute, University Karlsruhe, Hertz-Str. 16, D-76187 Karlsruhe, Germany*

AND WALTER MOONEY

*U.S. Geological Survey, 345 Middlefield Rd., M.S. 977, Menlo Park, California 94025*

## Abstract

We infer the fine structure of a sub-Moho boundary layer (SMBL) at the top of the lithospheric mantle from high-resolution seismic observations of Peaceful Nuclear Explosions (PNE) on super-long-range profiles in Russia. Densely recorded seismograms permit recognition of previously unknown features of teleseismic propagation of the well known  $P_n$  and  $S_n$  phases, such as a band of incoherent, scattered, high-frequency seismic energy, developing consistently from station to station, apparent velocities of sub-Moho material, and high-frequency energy to distances of more than 3000 km with a coda band, incoherent at 10 km spacing and yet consistently observed to the end of the profiles.

Estimates of the other key elements of the SMBL were obtained by finite difference calculations of wave propagation in elastic 2D models from a systematic grid search through parameter space. The SMBL consists of randomly distributed, mild velocity fluctuations of 2% or *schlieren* of high aspect ratios ( $\geq 40$ ) with long horizontal extent ( $\sim 20$  km) and therefore as thin as 0.5 km only; SMBL thickness is 60–100 km.

It is suggested that the SMBL is of global significance as the physical base of the platewide observed high-frequency phases  $P_n$  and  $S_n$ . It is shown that wave propagation in the SMBL waveguide is insensitive to the background velocity distribution on which its *schlieren* are superimposed. This explains why the  $P_n$  and  $S_n$  phases traverse geological provinces of various age, heat flow, crustal thickness, and tectonic regimes. Their propagation appears to be independent of age, temperature, pressure, and stress.

Dynamic stretching of mantle material during subduction or flow, possibly combined with chemical differentiation have to be considered as scale-forming processes in the upper mantle. However, it is difficult to distinguish with the present sets of  $P_n/S_n$  array data whether (and also where) the boundary layer is a frozen-in feature of paleo-processes or whether it is a response to an on-going processes; nevertheless, the derived quantitative estimates of the SMBL properties provide important constraints for any hypothesis on scale-forming processes. Models to be tested by future numerical and field experiments are, for example, repeated subduction-convection stretching of oceanic lithosphere (marble-cake model) and *schlieren* formation at mid-ocean ridges. It is also proposed that the modeling of the observed blocking of  $S_n$  and  $P_n$  propagation at active plate margins offers a new tool to study the depth range of tectonics below the crust-mantle boundary.

---

<sup>1</sup> Corresponding author; e-mail: Karl.Fuchs@gpi.uni-karlsruhe.de

Finally, the deduced schlieren structure of the SMBL closes an important scale gap of three to four orders of magnitude between structural dimensions studied in petrological analysis of mantle samples (xenoliths or outcrop of oceanic lithosphere) and those imaged in classical seismological studies of the lithosphere.

## Introduction

IT WILL BE SHOWN that the sub-Moho lithosphere possesses a heterogeneous fine structure of physical properties similar to the heterogeneities of the lower crust, and yet distinctly different from its crustal pendant. It is notable that both these heterogeneous zones above and below Moho were interpreted from the observation and analysis of scattered wavefields on densely spaced seismometer arrays. Both scattered wavefields are closely linked to the crust-mantle boundary. They reveal heterogeneities in the 0.5 km scale, whereas classical seismological investigations of the subcrustal lithosphere (inversion of travel times or of surface wave dispersion) image objects with dimensions of 10 to 100 km—e.g., mountain roots or thickness of lithospheric plates. This is far from the scale usually observed in geological/petrological field studies which encounter a high degree of heterogeneity. Petrological studies of mantle specimens (xenoliths or exposure of oceanic lithosphere) involve scales of less than 1/10 mm to 10 m (i.e.,  $10^{-7}$  to  $10^{-2}$  km). The scales covered by the seismological and petrological observations differ at least by three to four orders of magnitude.

We show that the seismic coda following a wave front can provide a resolution of the scales in between the two (i.e.,  $10^3$  cm versus  $10^6$  cm), if observed on appropriate high-resolution arrays. These seismic codas may consist of late-arriving signals or phases that have traveled on an extremal travel time path as governed by Fermat's law. Likewise, these codas consist of scattered energy, incoherent from station to station, from objects having dimensions on the order of the seismic wavelength or smaller.

The seismic observations of powerful Peaceful Nuclear Explosions (PNE) (Egorkin and Pavlenkova, 1981; Mechie et al., 1993) on super-long-range profiles ( $>3000$  km) with a station spacing of only 10 km allowed the identification of a high-frequency scattered phase. The coda was seen consistently to have a duration of  $\sim 10$  sec, with its front traveling at a group velocity equivalent to uppermost mantle material (Ryberg et al., 1995).

Several theories have been proposed to explain the efficient propagation of high-frequency energy

over large distances of more than 3000 km. For an overview see Sereno and Orcutt (1985, 1987). These theories include models with scatterers in the lower crust and/or upper mantle (Gettrust and Frazer, 1981; Menke and Richards, 1983; Richards and Menke, 1983; Menke and Chen, 1984; Mallick and Frazer, 1990; Ryberg et al., 1995; Thybo and Perchuc, 1997; Ryberg and Wenzel, 1999; Tittgemeyer, 1999; Tittgemeyer et al., 1999; Ryberg et al., 2000b). An alternative model was proposed by Morozov (2000, and references therein), who attempted to revive the whispering gallery model with all the heterogeneities in the lower crust. In this paper we will show by finite difference experiments that this concept does not match the observations of the  $P_n$  phase; second, the whispering gallery does not explain the selective propagation of high-frequency energy over distances up 10,000 wavelengths; third, since reflective lower crust is not present everywhere, the whispering gallery model does not produce a globally observed  $P_n$  and  $S_n$  phase with high-frequency coda, and finally there is no whispering gallery propagation in high-heat-flow regions. In short, the whispering gallery concept explains neither the PNE observational characteristics nor the global observation of  $P_n$  and  $S_n$  propagation. For a detailed reply to Morozov (2000), see Ryberg and Wenzel (2002) and Tittgemeyer et al. (2002).

Our preferred interpretation, described below, satisfies the described characteristics of the observed  $P_n$  and  $S_n$  propagation. They are trapped in a forward scattering waveguide, which is considered as a sub-Moho boundary layer (SMBL) with a thickness ( $L$ ) of 60–100 km, starting directly below the Moho and extending into the upper mantle. Various structural properties of the boundary layer point to formative processes having a strong horizontal component.

The discovery of this lithospheric boundary layer with thin horizontal schlieren<sup>2</sup> is of global significance because the seismic signals propagated in it are a global phenomenon (e.g., Molnar and Oliver, 1969). The deduced boundary layer provides a physical basis for the global observation of the classical seismological  $P_n$  and  $S_n$  phases. The interrup-

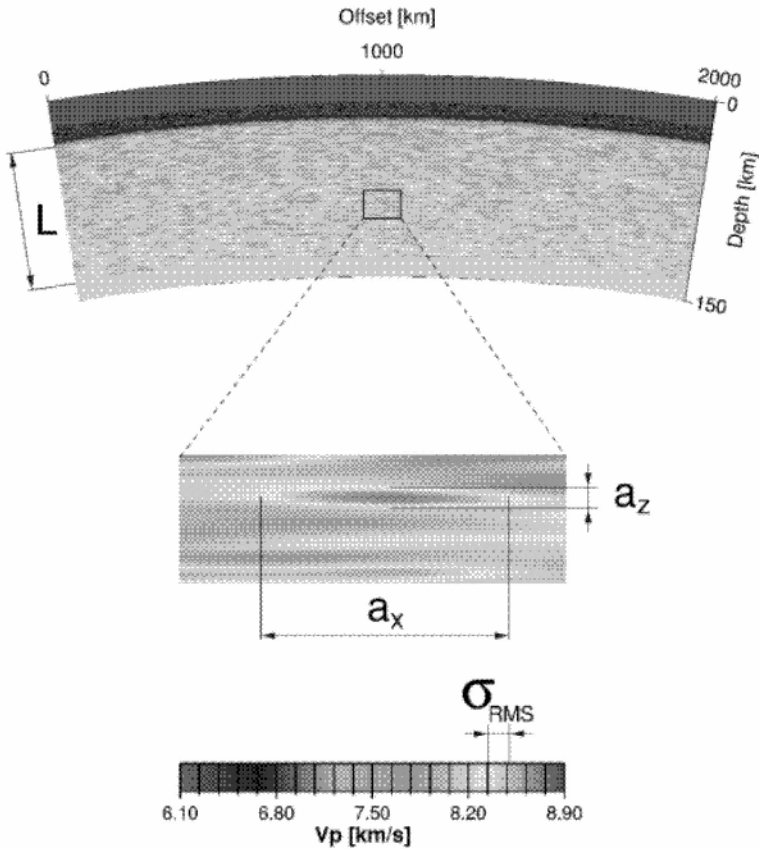


FIG. 1. The sub-Moho boundary layer. Parameter space of the fluctuating upper mantle waveguide: vertical and horizontal autocorrelation length,  $a_z$  and  $a_x$ , respectively; thickness of the waveguide  $L$ ; and RMS standard velocity deviation  $\sigma_{\text{RMS}}$ .

tion of their propagation at plate boundaries provides a new constraint on the depth range of active tectonic processes at these margins. Many attributes of the boundary layer point toward a significant presence of dynamic processes near the crust-mantle boundary.

### The Sub-Moho Boundary Layer (SMBL)

The release of formerly restricted data from previously confidential observations of Peaceful

Nuclear Explosions (PNE) in the former USSR led, among other things, to the discovery of a sub-Moho boundary layer with schlieren-like fluctuations of seismic velocities in the lithospheric mantle directly below the Moho (Ryberg et al., 1995; Tittgemeyer et al., 1996; Wenzel et al., 1997; Ryberg and Wenzel, 1999). These velocity fluctuations were deduced from the analysis of PNE data that were recorded on linear arrays with apertures of several thousand kilometers and station separation as small as 10 km, a scale of experiment not previously achieved.

The interpretation of the high frequency  $P_n$  phase led to the development of the SMBL model that has a thickness ( $L$ ) of ~60–100 km (Fig. 1). In a randomly fluctuating velocity model with a velocity variance  $\sigma = 2\%$  the heterogeneities are strongly extended subhorizontally and resemble “schlieren” in form. Their horizontal and vertical extents (mea-

<sup>2</sup>Schlieren occur in some igneous rocks as irregular streaks or masses that contrast with the rock mass but have transitional boundaries. They may represent segregations of dark or light minerals or altered inclusions, elongated by flow. The word is derived from the German for a flaw in glass due to a zone of abnormal composition (AGI, 1972).

sured by their autocorrelation length) are  $a_x = 20$  km and  $a_z = 0.5$  km, respectively, corresponding to an aspect ratio  $a_x/a_z$  of 40. These quantitative estimates of the parameters describing the boundary layer and its internal fluctuations were obtained by numerical simulations of wave propagation in the SMBL model matching the observed PNE-record sections on the super long-range profiles.

### *SMBL in light of seismic waves*

There are two principal seismic observations that define the properties of the sub-Moho boundary layer. The first is the absence of backscattering from the SMBL at near-vertical incidence. The second is the ability of the SMBL to propagate the high-frequency part of the seismic signal, incident upon the Moho at critical angle, horizontally to teleseismic distances of more than 3000 km (Tittgemeyer et al., 2000). We discuss each below.

*Near-vertical incidence.* At near-vertical incidence, the lithospheric mantle including the SMBL becomes non-reflective or transparent for signals typically used in seismic exploration (5–50 Hz). This characteristic contrasts with the highly reflective lower crust. This is a consequence of smoother fluctuations in the sub-Moho region compared to those in the lower crust. In other words, fluctuations in the boundary layer have lost part of their short-scale properties. The globally documented (Mooney and Brocher, 1987) coincidence of the “reflection” Moho (as the lower boundary of the backscattering lower crust) with the original “refraction” Moho (as a jump in wave velocities, i.e., composition) must be recognized as a consequence of the smoothness of the fluctuations in the boundary layer. The discovery of the SMBL implies that the Moho has a previously unrecognized attribute: in addition to a sharp increase in seismic velocities, composition, and density, it is the boundary between heterogeneities with different scale-length distributions. The shorter structural scale lengths that cause strong backscattering in the lower crust at about 10 Hz are absent in the uppermost mantle, such that the SMBL becomes transparent at near-vertical incidence. Within the observed band-width, this corresponds to a change from almost self-similar distribution of heterogeneities in the lower crust to non-self-similar distribution in the topmost mantle. We interpret this as evidence for the operation of two different processes, one in the crust, the other in the uppermost mantle. This means that the Moho can be regarded as a process boundary.

*Critical angle of incidence on crust-mantle boundary.* At the critical angle of incidence on the crust-mantle boundary, the SMBL becomes a frequency-selective waveguide generating a high-frequency  $P_n$  wave with a clear coda. This observation comes from the highly successful PNE program in the former USSR during 1970–1990 which was based on an unprecedented design of seismic observations. The more than 300 mobile seismic stations covered the entire length of the profile (>3000 km) as one deployment, and recorded the wavefield generated by PNE shots with sufficient energy to reach the ends of the profiles. This permitted the observation of unusual properties of the high-frequency  $P_n$  coda as a forwardly scattered energy band. The  $P_n$  band travels behind the wave front, returning from the mantle transition zone with its discontinuities to a depth of about 660 km (Mechie et al., 1993).

The  $P_n$  band, as observed for the first time on a large-aperture linear array, is especially clearly recognized on high-pass filtered ( $f > 5$  Hz) record sections, as shown on the Quartz-profile (see Fig. 2). SP323 is on the southeastern end and the line traverses the Urals to the northwest. Apart from the coda band, which is incoherent at a station separation of 10 km, the  $P_n$  band shows the following characteristics: (1) After separation from the direct P-wave signal at a distance of 1500 km, the teleseismic  $P_n$  phase is recognized as the beginning of a band of coda energy, broadening with distance, that can be consistently followed from station to station despite the incoherence of the coda. (2) The front of the band travels with a velocity of 8.0–8.1 km/s, slightly increasing with distance. (3) The scattered teleseismic  $P_n$  phase develops as a linear continuation out of the short-offset, headwave-like diving wave (Tittgemeyer et al., 2000) with practically the same apparent velocity and intercept-time. Since the time of Mohorovicic (1910), this short-offset  $P_n$  has been used to define the crust-mantle boundary. In view of these observed characteristics and also because the transparency of the SMBL starts at the Moho, the top of the mantle boundary layer is closely connected to the Moho. (4) Another observational discriminant is the amplitude-frequency distribution between the first-arriving direct P phase and the  $P_n$  phase: in the high-pass filtered section, most of the high-frequency energy is traveling with the  $P_n$  phase. In global seismology, these phases have been observed with extremely high frequencies (up to 30 Hz) at large distances (up to 40°, Walker, 1977, 1981). The corresponding  $S_n$  phase with sim-

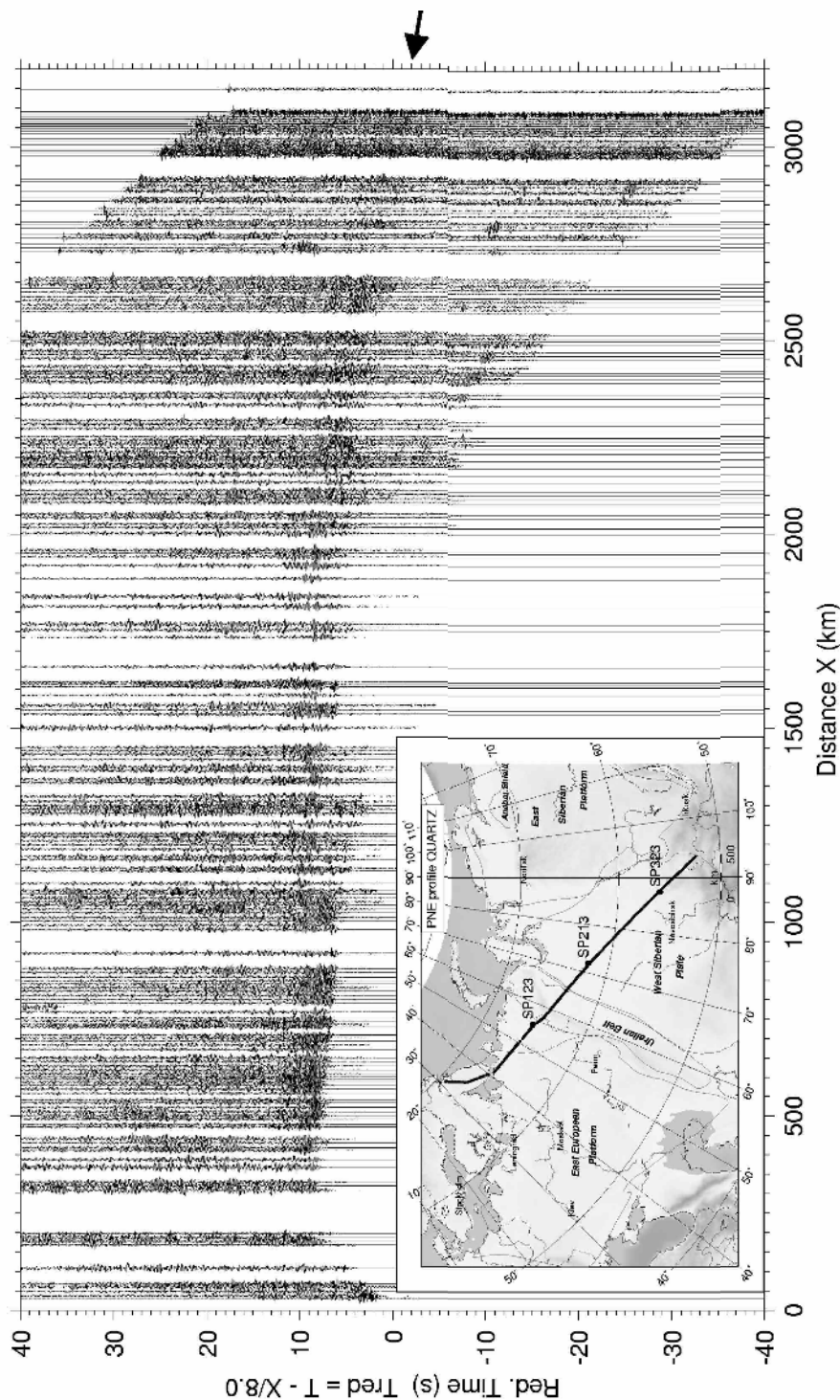


FIG. 2. P-wave seismogram section PNE profile Quartz. High-pass filtered ( $> 5$  Hz) for SP 323 recorded to the northwest on the PNE profile Quartz. Trace-normalized seismograms of the vertical component with reduction velocity of 8.0 km/s. The strong band marked by an arrow is the high-frequency teleseismic  $P_n$  phase. The map in the inset illustrates the station distribution along the profile (after Ryberg et al., 1995).

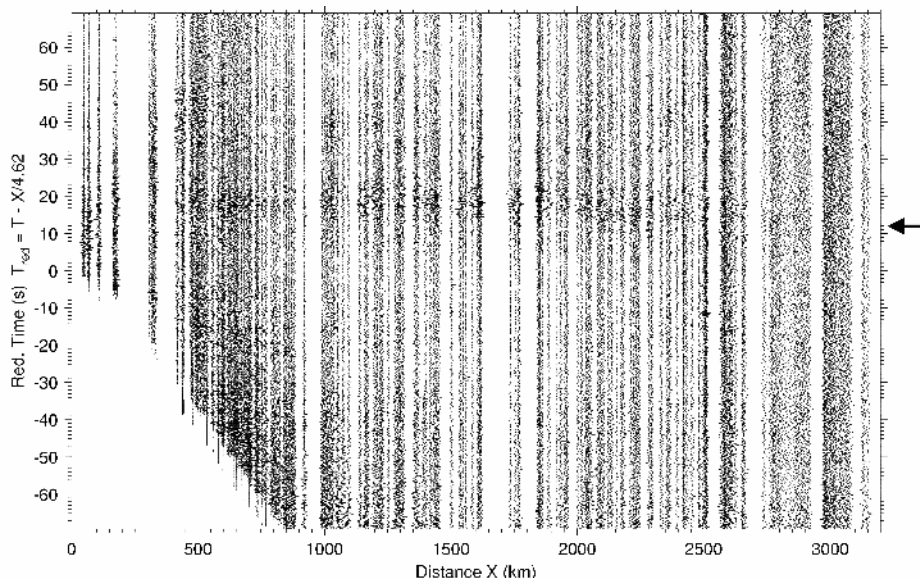


FIG. 3. S-wave seismogram section PNE profile Quartz. Unfiltered section for SP 323 recorded to the northwest on the PNE profile Quartz. Trace-normalized seismograms of the horizontal radial component with a reduction velocity of 4.62 km/s. The band marked by an arrow is the high-frequency teleseismic  $S_n$  phase from the same shot on the same deployment as the P-section in Figure 2. Although the section is unfiltered and S-phases are usually weaker from explosions than from earthquakes, the high-frequency  $S_n$  is the only visible phase.

ilar properties can be seen even on the unfiltered horizontal radial component record section as a high-frequency band (Fig. 3; Tittgemeyer, 1999). Although the section is unfiltered and S-phases are usually weaker from explosions than from earthquakes, the high-frequency  $S_n$  is the only visible phase.

#### *Matching observed and simulated seismograms—a grid search through parameter space*

Simulations of wave propagation through a realistic continental lithosphere comprising the crust and sub-Moho boundary, with its incorporated statistical distribution of velocity fluctuations, require a special finite difference (FD) code for 2D models. Such a code has been developed (Ryberg and Tittgemeyer, 2000; Ryberg et al., 2000a, 2000b) to run on a fast modern supercomputer.<sup>3</sup> A grid search for the optimum matching of observed and simulated record sections was performed by a systematic

change of the following parameters that describe the properties of the SML:  $a_z$  and  $a_x$ , the vertical and horizontal autocorrelation lengths, respectively;  $L$ , thickness of the waveguide; and  $\sigma_{\text{RMS}}$ , standard deviation of the velocity (Fig. 1). Many results have been published (Tittgemeyer, et al., 1999; Fuchs et al., 2002). In Figures 4 and 5 we present two important examples.

The sensitivity of the simulated record sections to slight modifications of the model parameter  $\sigma$ , the variance of the velocity fluctuations, is demonstrated in Figure 4. All other parameters are already set at their deduced optimal value:  $a_x = 20$  km,  $a_z = 0.5$  km, and  $L = 60$  km. The velocity fluctuations were overlaid on the background IASPEI model (Kennett et al., 1995) from 30 to 130 km depth. The case at the top ( $\sigma = 0\%$  without fluctuations) is followed by examples with  $\sigma = 1\%$ ,  $2\%$ , and  $3\%$ .

*Without velocity fluctuations.* Without velocity fluctuations most of the energy is in the direct P wave. The “whispering gallery” (WG) phases (e.g., Menke and Richards, 1980) are weakly developed in comparison to the direct P phase. There is no frequency difference between direct P and the whis-

<sup>3</sup> The CRAY T3E/900MHz computer with 512 parallel processors and 128 Mb/processor at the German High Performance Computer Centre in Stuttgart.

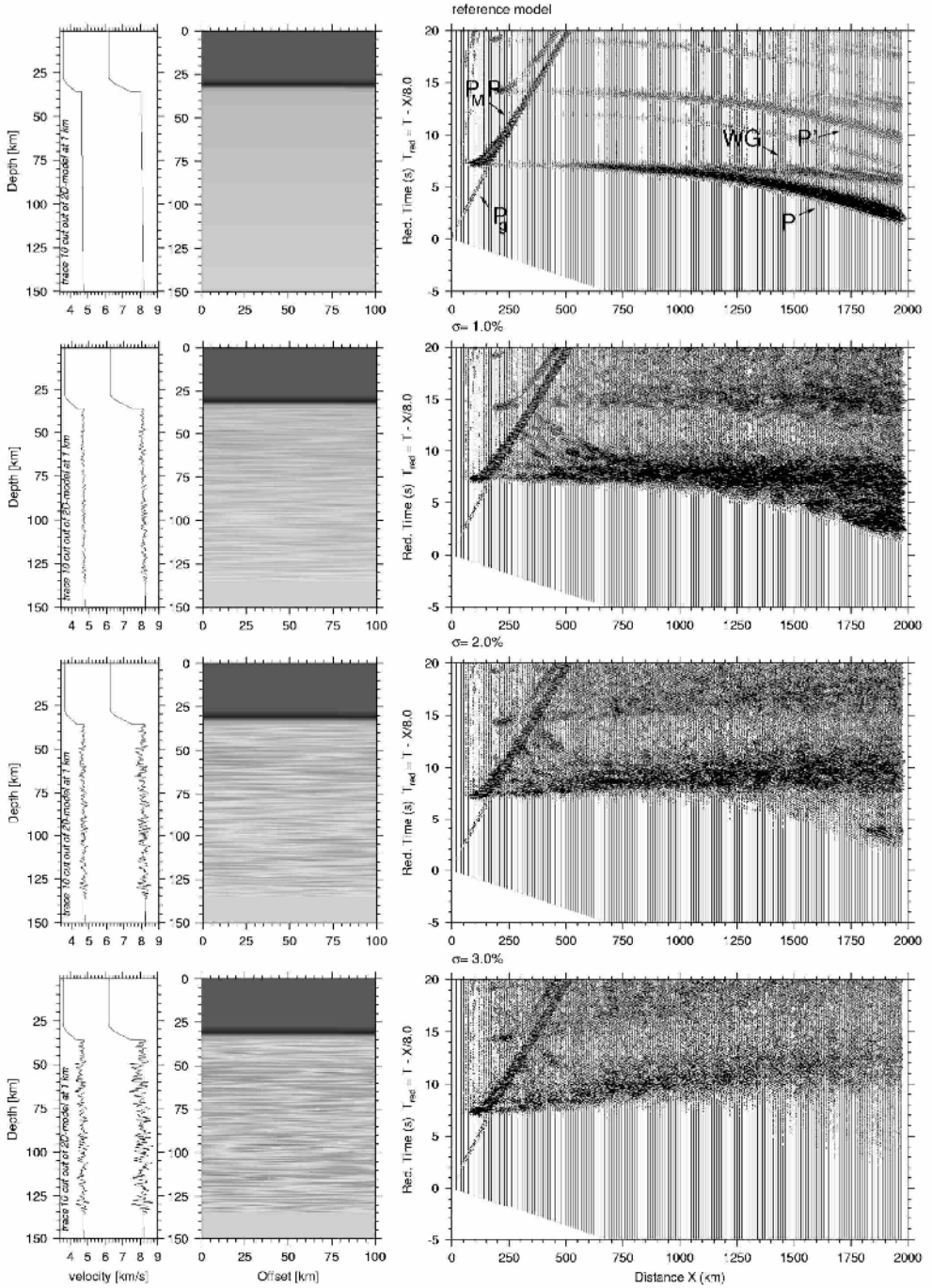


FIG. 4. Grid search through parameter space; sensitivity to changes of velocity variance. Synthetic seismograms for various stochastic models (left part of figure) of the upper mantle. The statistics on which the models are based varies only in the variance  $\sigma_{\text{RMS}}$  of the velocity fluctuations; i.e.,  $\sigma_{\text{RMS}} = 0, 1, 2, 3\%$  (from top to bottom). The other parameters are kept unchanged at their optimum values:  $a_z = 0.5$  km;  $a_x = 20$  km;  $L = 100$  km (after Ryberg et al., 2000b). Row 1: Model without fluctuations; no coda. Most of the energy is in the Fermat P phase (contrary to observations); no frequency selective enhancement. Row 2:  $\sigma_{\text{RMS}} = 1\%$ ; too much energy on Fermat Branch. Row 3:  $\sigma_{\text{RMS}} = 2\%$ ; optimum case. Row 4:  $\sigma_{\text{RMS}} = 3\%$ ; too much energy in  $P_n$ ; Fermat P ray disappears completely.

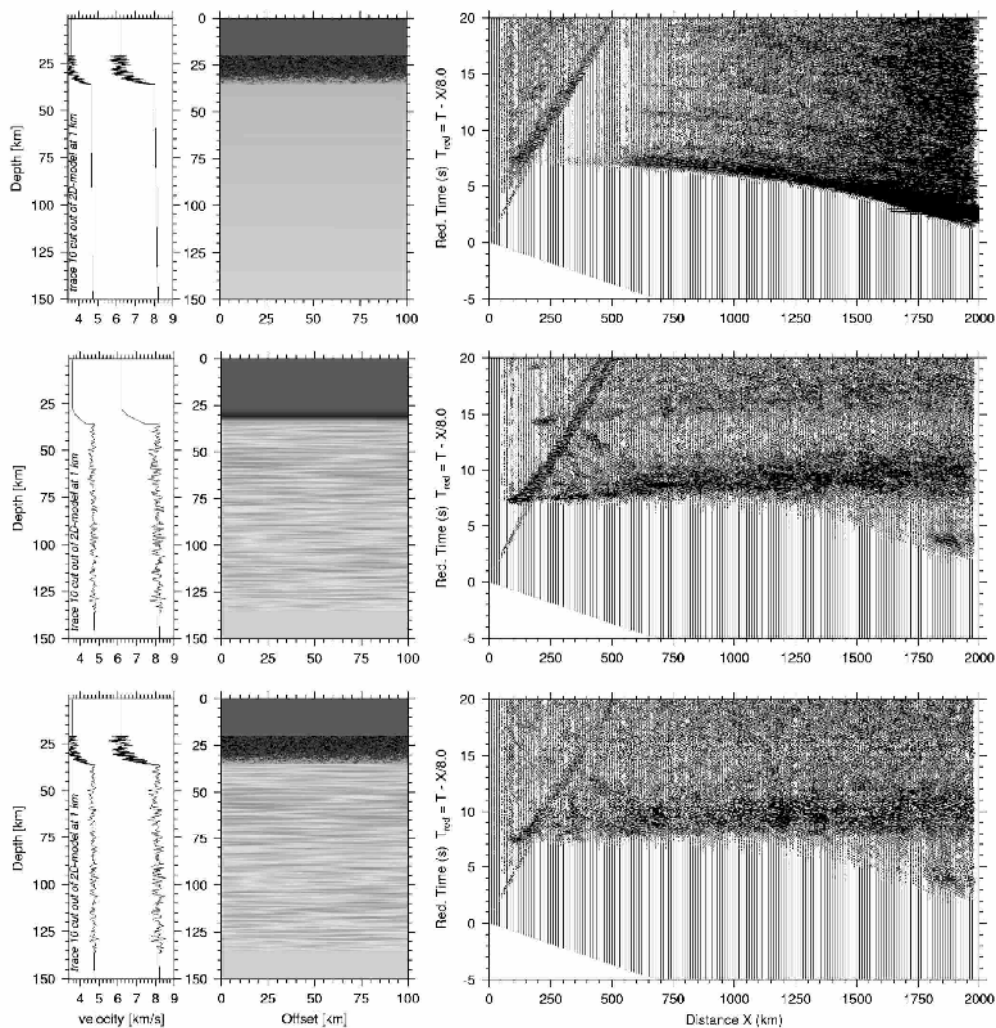


FIG. 5. Grid search through parameter space; influence of lower crust on  $P_n$  (after Ryberg et al., 2000b). Top: lower-crustal heterogeneities on top of IASPEI mantle (Kennett et al., 1995). The energy remains in the direct wave; the  $P_n$  phase is not generated. Middle: case of Figure 4 (Row 3), fluctuating (2%) mantle without lower crust. Bottom: lower-crustal heterogeneities on top of fluctuating mantle. In comparison with the middle row, note that there is no visible influence of lower-crustal heterogeneities.

pering gallery phases. Both features do not comply with the observations.  $P'$  is the surface multiple reflection of the refraction phase.

$\sigma = 1\%$ .  $P_n$  can be recognized, but the velocity fluctuations are not yet strong enough to sufficiently trap high-frequency amplitudes to be propagated in the waveguide.

$\sigma = 2\%$ . This variance allows enough low-frequency P-wave energy to penetrate into the mantle

beneath the boundary zone. The amplitude ratio of  $P_n/P_{\text{direct}}$  matches best the observations (see Fig. 2).

$\sigma = 3\%$ . The velocity fluctuations are too strong. Only a small portion of the direct P-wave can penetrate the boundary layer. Most of the incident P-energy is deflected to travel as  $P_n$  in the boundary layer.

It should be noted that the duration and intensity of the coda is extremely sensitive to  $\sigma$  and less to the



aspect ratio  $a_x/a_z$ . The only requirement is that the aspect ratio must be larger than 40.

**Lower-crustal heterogeneities.** Figure 5 shows that lower-crustal heterogeneities cannot be responsible for the generation of the observed band of the scattered  $P_n$  phase with its coda (Ryberg et al., 2000b). The reflective lower crust on top of model IASPEI (Kennett et al., 1995; Figure 5, top), but without the SMBL, does not generate a  $P_n$  phase; the heterogeneities of the lower crust destroy the weak whispering gallery phase, and the multiple P-direct reflections from the free surface. Instead the lower-crustal heterogeneities generate a broad coda immediately following the direct P first arrival. All this is incompatible with the observations of the  $P_n$  phase. Figure 5 (middle), in comparison, is the optimal model with the sub-Moho boundary layer, here without lower-crustal heterogeneities. The same case with both the heterogeneous lower crust and SMBL is displayed in Figure 5 (bottom). The introduction of the lower crust does not destroy the  $P_n$  phase, but clearly wipes out the surface reflections.

3D simulations to 2000 km distance have not yet been carried out. We do not expect dramatic changes in the required geometry of the schlieren; however, from our experience in the step from 1D to 2D modeling, a possible decrease of the required velocity variance cannot be excluded.

To summarize, we have shown, even independently of the PNE data, that long-range high-frequency propagation of  $P_n$  with a long coda requires a sub-Moho waveguide. In other words, wherever a  $P_n$  or  $S_n$  coda is observed at teleseismic distances, it requires the presence of such a waveguide.

### Global Significance of the Sub-Moho Boundary Layer

The discovery of the sub-Moho boundary layer, and the quantitative definition of its modest (2%) velocity fluctuations as well as its role as a waveguide in teleseismic  $P_n/S_n$  propagation, is of global significance for three reasons. First, the high-frequency propagation of  $P_n$  and  $S_n$  is a well established global phenomenon, known as early as 1935 (e.g., Linehan, 1935). Second, the SMBL can serve as the physical basis for  $P_n/S_n$  propagation, because the forward scattering is independent of the background model (governed by age, temperature, pressure, and other parameters such as tectonic regime). Last but not least, the SMBL is connected to another global phenomenon, the Mohorovicic discontinuity.

Since processes at active plate margins block  $P_n/S_n$  propagation, they must also affect waveguide properties of the SMBL. The study of the blocking mechanism offers a new tool to study the depth range of crustal tectonic features into the mantle. Furthermore, the scales of fluctuations in the boundary layer narrow the gap between seismological structures and geological and geochemical observations of the fine structure of mantle rock.

### SMBL—physical model for global $P_n/S_n$ propagation

Although array observations with apertures comparable to the PNE observations on super-long-range profiles do not exist outside Russia, either on the continents or in the oceans,  $P_n$  and  $S_n$  phases have been widely studied in global seismological research. Short-period P had been used even in the 1920s to define the 20° discontinuity (Byerlee, 1926) as the intersection between P and the higher-velocity phases from the mantle transition zone (Gutenberg, 1954; Lehmann, 1964). Note that in Figure 2, the low frequency signals from the transition zone have been removed by the high-pass filter. Despite the mixture of seismometer types and their irregular spatial distribution, the  $P_n$  and  $S_n$  phases were consistently observed even as a later arrival. This points indirectly to a remarkably efficient wave propagation mechanism.

In a related study, Molnar and Oliver (1969) applied the  $S_n$  observations from the Worldwide Standard Seismic (WWSS) network to map active plate boundaries. Their map of global  $S_n$  propagation, updated with the network of teleseismic  $P_n$  observations on PNE profiles, is shown in Figure 6. Tracing  $S_n$  between earthquake source and single stations, they found that the short-period teleseismic  $S_n$  phase propagated efficiently almost everywhere: over continents, oceans, and even across passive continent-ocean boundaries. The propagation of  $S_n$  is only blocked at three types of active plate margins: mid-ocean ridges, subduction zones, and in some cases also at continental transform faults.

$S_n$  and  $P_n$  traverse geological provinces that differ in age, crustal thickness (pressure), heatflow (temperature), and tectonic regime (stress), both in the oceans and on continents. The independence of effective  $P_n/S_n$  propagation through plate interiors from age and physical conditions demonstrates that the SMBL is not just a regional feature of the Russian platform.

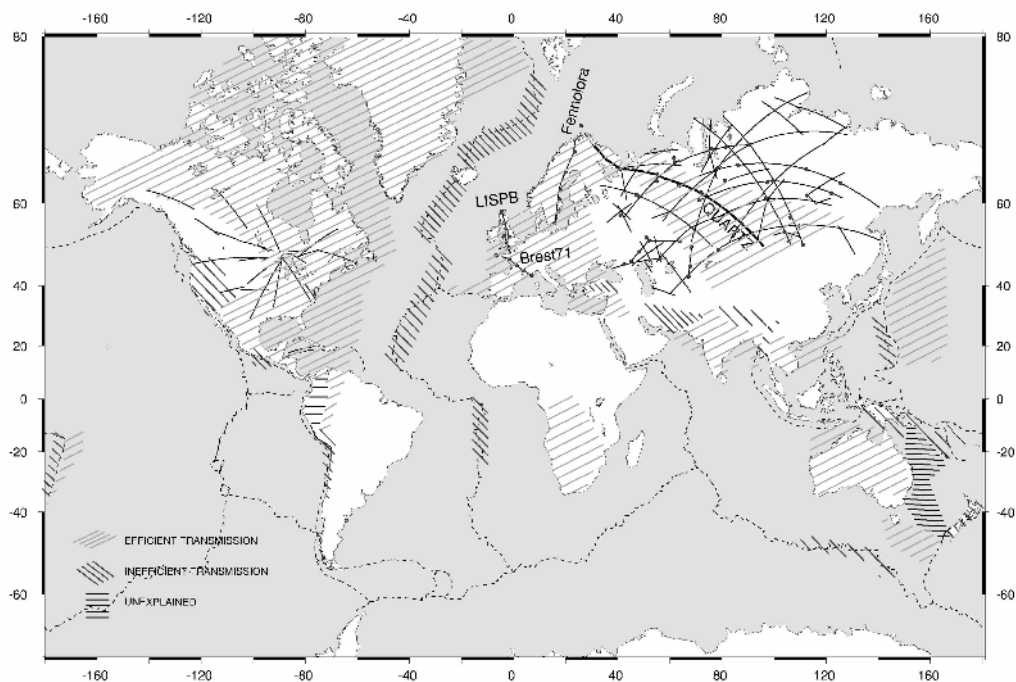


FIG. 6. World map of  $S_n/P_n$  propagation (after Molnar and Oliver, 1969). The map is updated with the network of teleseismic  $P_n$  observations on PNE profiles, and displays global properties of  $S_n/P_n$  propagation. Right-dipping hatches mark regions of inefficient propagation; left-dipping hatches stand for efficient propagation; horizontal hatches are regions of unclear classification.

Indeed, it can be shown that the waveguide properties are to a large extent independent of the background. We have already demonstrated by numerical experiments that the SMBL is an effective waveguide, even if the fluctuations are riding on a sub-Moho low-velocity zone like those induced in high heat-flow regions (Tittgemeyer et al., 1996; Sobolev et al., 1997). The vertical and horizontal autocorrelation lengths and the thickness  $L$  may change, but a fluctuating waveguide must exist; otherwise  $P_n$  and  $S_n$  would not be a globally observed phenomenon.

#### *Schlieren-generating processes*

What kind of processes could possibly generate the SMBL and its internal schlieren-like fluctuations with its characteristic structural dimensions of physical properties? This is the most obvious question to be asked, once the existence of the boundary layer has been recognized.

To this point we have used the term “processes” in the widest sense possible as “processes that cre-

ate schlieren-like fluctuations.” There are probably two end-member models for the creation of schlieren, however. First, they can be the result of chemical differentiation or fractionation of the lithospheric mantle during partial melting. Second, schlieren can form during deformation by creep or laminar flow. It can, of course, be a mixture of both processes, as suggested, for example, in the marble-cake model (Allegre and Turcotte, 1986).

Schlieren as a global phenomenon can be interpreted as a result of deformation in ductile material, analogous to the concept of lower-crustal reflectivity. Inhomogeneities within the upper 100 km of the mantle are stretched to schlieren when significant strain causes elongation of the material. Inhomogeneities would be expected. They exist at mid-ocean ridges as the result of various spreading episodes. They are generated in collapsing orogens, with crustal roots involved, during crustal collision and during extension, when deeper mantle material rises. Velocity fluctuations of 2–10% are pertinent in the inventory of mantle material (Mainprice and

Silver, 1993; Sobolev et al., 1997). Contrary to lower crustal material, the mantle shows smoothed material mixtures, probably due to the higher temperatures, and hence no vertical reflections are observed.

Large strains in the oceanic lithosphere at a high geothermal gradient can occur close to mid-oceanic ridges. Large strain in ductile material beneath the continental Moho is also conceivable if geothermal gradients are high. In this case, the entire strength of the lithosphere comes from the brittle upper crust without any mantle contribution. When the temperature drops during later tectonic episodes, the schlieren are frozen into the lithosphere.

Lower-crustal lamellae are generated by postorogenic collapse that allows large-scale ductile flow at elevated temperatures. Consequently lamellae are mostly found at sites of equilibrated former orogens, such as in the Variscan Mountains. Therefore, the laminated lower crust is not a global feature. In contrast, the SBL as a global phenomenon points to the fact that its generating deformation process occurred almost everywhere beneath the Moho at least at some time in Earth history. The Moho is a global feature because the Earth is chemically differentiated into crust and mantle on a global scale. The SBL is a global feature because sub-Moho flow and associated deformation always occurs during the formation of the oceanic lithosphere; practically all continents are pushed across the planet by plate-tectonic forces and experience elevated temperatures at some point in their history.

With the present sets of  $P_n/S_n$  array data, it is difficult to distinguish whether, and also where, the boundary layer is a frozen-in feature of paleo-processes, or whether it is a response to ongoing processes. Most important for the answer, however, are the new quantitative assessments of SBL parameters. For the first time, we provide measures of structural dimensions as well as of scatterer strength in an upper zone of the mantle lithosphere that appeared until recently to be devoid of any significant structure. All acceptable processes for creating schlieren have to take into account the fact that the boundary layer is limited in thickness, and that the fluctuations start directly below the Moho in the data sets available to us. All things considered, differential horizontal deformation between crust and mantle near the Moho is the most likely explanation for the creation of seismic velocity fluctuations within the SBL.

### Blocking of $P_n/S_n$ and Processes at Sub-Moho Plate Margins

Molnar and Oliver (1969) used the blocking of  $S_n$  phases to map active plate margins. This blocking of  $S_n$  propagation at mid-ocean ridges, subduction zones, and in part at continental transform faults must be compatible with the hypothesis that the SBL is a waveguide for platewide  $S_n$  and  $P_n$  propagation. Numerical experiments have shown that the disappearance of the  $P_n$  phase at subduction zones can be understood by bending the schlieren within and together with the boundary layer. This keeps the energy in the subducting slab and prevents the crossing of this active margin. The physical cause for the blocking by major tectonic features has received little attention. Since the global studies by Molnar and Oliver (1969), several regional studies following the same philosophy were conducted for the Indian shield and Tibetan Plateau (Ni and Barazangi, 1983), for the Nazca plate and across the Altiplano in South America (Chinn et al., 1980), for the Banda Arc (Barazangi et al., 1977), for southern Africa (Nyblade et al., 1996), for the Turkish and Iranian Plateaus (Kadinsky-Cade et al., 1981) and for China (Rapine et al., 1997), for the Middle East (Rodgers et al., 1997), and for the Africa-Iberia plate boundary (Calvert et al., 2000). The efficiency of  $S_n$  and  $P_n$  propagation is also of importance in the Comprehensive Test Ban Treaty (CTBT) for discrimination of earthquakes and explosions (e.g., Kennett, 1989).

The blocking of  $S_n$  propagation at mid-ocean ridges has two likely explanations. Anelastic damping of the  $S_n$  phases in an upwelling hot, low  $Q$  asthenosphere is certainly a main cause for the disappearance of the  $S_n$  phase. But the ridges are also the place where new oceanic lithosphere is created and probably where the  $P_n/S_n$  waveguide is generated in the SBL. However, since the SBL requires a certain thickness before it can transmit  $P_n/S_n$  to teleseismic distances, we suggest that effective transmission can only start once oceanic lithosphere has cooled and reaches a critical thickness. Assuming that the thickness ( $L$ ) is the same in the oceans as on the continents ( $L \sim 60$ – $100$  km), the efficient transmission would start at a distance from the ridge with an age of  $\sim 50$  to  $100$  Ma (Turcotte and Schubert, 1982, p. 164). Passive-array observations at teleseismic distances parallel to the mid-oceanic ridges on "isochronal" profiles would provide an important test of the proposed SBL model for the

oceans. If applicable, they would also give new constraints on age-dependent lithospheric thickness and formation of the oceanic lithosphere.

Continental transform faults show a mixed behavior on the world map of  $S_n$  propagation. The North Anatolian fault in Turkey and the San Andreas fault in the United States block  $S_n$  transmission. In contrast, the Dead Sea transform fault is characterized by efficient  $S_n$  transmission (however, Rodgers et al., 1997, found blocking of  $S_n$ ). A very special case is the New Zealand Alpine fault in the 1969 Oliver and Molnar map. It displays efficient transmission of  $S_n$  on paths from the east and inefficient transmission on paths from the west.

Continental transform faults are the margins where lithospheric plates slide past each other horizontally. Studies of seismicity, surface geology, the stress field, heat flow, etc. are all the product of the tectonic events that have modified the crust. However, little is known regarding how tectonic behavior continues below the Moho. The existence of defects in the schlieren waveguide in the shallow mantle along continental transform faults could be a reliable measure of interaction between lithospheric mantle and crust at plate margins.

Modern higher resolution  $S_n$  data for paths across transform faults should also discriminate between the properties of the topmost mantle of various sections of the transform faults. If schlieren are a result of domain-like variations of the preferred orientation of olivine crystals, and if they are bent around a vertical rotation axis, guided  $P_n/S_n$  propagation should follow the fast axis of P wave anisotropy parallel to the relative motion along the transform fault (e.g., Polet and Kanamori, 2001). We foresee that the faster motion leads to more efficient orientation parallel to the fault plane and will therefore result in more efficient blocking. This may be an explanation for the different behavior of the San Andreas Fault compared with the Dead Sea Fault.

## Summary and Conclusions

The newly discovered fine-scale velocity fluctuations in the SMBL have important implications for the study of the dynamics of the mantle lithosphere. The most important points are briefly summarized, together with possible tests of tectonic models.

*Global features of the sub-Moho mantle.* We have shown that  $P_n/S_n$  propagation in the boundary layer is essentially independent of whether the propagation is in hot or in cold lithosphere. Although the

database outside the PNE experiments does not allow detailed modeling of the sub-Moho layer, we propose to take its existence as the basis for the observed worldwide  $P_n/S_n$  propagation.

*Moho—a boundary separating distinct processes.* The Moho is a boundary below which the mantle material has lost distinctly short-scale-length fluctuations. This causes the sub-Moho boundary layer to become transparent on vertical incidence of seismic waves, whereas at the same time being an efficient waveguide to teleseismic distances for high-frequency  $P_n/S_n$  propagation. Since fine structure is an expression of processes, we take this newly recognized property of the Moho as a sign of change in processes, and consequently the SMBL as a zone generating the particular schlieren-like fluctuations with specific measures of structural dimensions and magnitude of material (velocity) variances.

*Constraining scale-forming processes.* Our modeling of  $P_n/S_n$  propagation provides not only identification of the SMBL, but also the first quantitative measures of its thickness and its internal properties. All proposed scale-forming processes have to be tested against these new measures.

Although we cannot exclude the formation of the material fluctuations by heterogeneous refractory depletion of the top part of the lithospheric mantle, there are strong indications that dynamic processes play a major role in the formation of the sub-Moho boundary layer. The high aspect ratio, larger than 40, of spatial properties points to a strong stretching process, and the velocity variance of 2% is suggestive of a preferred orientation of anisotropic olivine crystals. This implies formation of the schlieren in the waveguide during a process of flow or creep in a zone (~60–100 km thick) near the crust-mantle boundary.

*A new tool to study sub-Moho tectonic processes.* Mapping of the sub-Moho boundary layer offers a new tool for the exploration of the depth range of tectonic processes reaching into the mantle. Since the boundary layer extends to 60–100 km below the Moho, any processes reaching this depth could possibly effect the boundary layer and its waveguide. An important aspect is the blocking of the  $P_n/S_n$  phases at plate boundaries. Although the formation of the fluctuations in the boundary layer cannot be dated—at present we cannot distinguish between paleo- and present processes, ongoing processes at plate margins block the propagation of both phases. Future studies must investigate how these processes affect the boundary layer, its thickness, the orienta-

tion of the schlieren, and the variance of the velocity fluctuations.

*Unifying the scale length for seismological and petrological studies.* The dimensions of the fluctuations in the SMBL fill an essential observational gap between structural dimensions in petrological and in classical seismological studies of lithosphere structures. This gap has prevented testing of models on schlieren-forming processes.

The marble-cake model (Allegre and Turcotte, 1986) has been proposed to explain the frequency distribution of thicknesses of pyroxenitic schlieren observed in a peridotitic oceanic lithosphere exposed in the Lherzo massif in the Pyrenees. Starting with a two-component oceanic lithosphere generated at a mid-ocean ridge, their model produces thin schlieren by shear and normal straining of the subducted slab in repeating convective cycles. The resulting schlieren structure is repeatedly and partially destroyed at mid-oceanic ridges while new oceanic lithosphere is generated. They showed that this process generates the distribution of schlieren thickness in the centimeter to meter-range. In a grand view, their model attempts to connect the seismologically measured km scales of the lithosphere to the cm scale of lherzolite schlieren. We believe that the SMBL presented in this paper is also a physical manifestation of the marble-cake process at intermediate scales that will serve to bridge this gap.

### Acknowledgments

The Deutsche Forschungsgemeinschaft supported this investigation through grants KA 1347/1-4 and RY 12/2-2. KF and TR acknowledge support for their visits to the U.S. Geological Survey, Menlo Park, CA. MT thanks the Max Planck Institute at Leipzig, in particular Dr. F. Kruggel, for his patience with regard to MT's geophysical research activities. The numerical calculations have been supported by the High-Performance Computer Center in Stuttgart. We appreciate permission to use the PNE data made available by GEON, Moscow and the many fruitful discussions with its Director, Dr. L. Solodilov, and Dr. A. V. Egorkin. Thanks also are due to the reviewers who helped with their constructive criticism to improve the content as well as the English. We especially appreciate the very intense review and advise for improvement by Ron Clowes.

### REFERENCES

- Allegre, C., and Turcotte, D. L., 1986, Implications of a two-component marble-cake mantle: *Nature*, v. 323, p. 123–127.
- AGI, 1972, Glossary of geology: Alexandria, VA: American Geological Institute.
- Barazangi, A., Oliver, J., and Isacks, B., 1977, Relative excitation of the seismic shear waves Sn and Lg as a function of source depth and their propagation from Melanesia and Banda arcs to Australia: *Ann. Geofis.*, v. 30, p. 385–408.
- Byerlee, P., 1926, The Montana earthquake of June 28, 1925: *Bulletin of the Seismological Society of America*, v. 16, p. 209–265.
- Calvert, A., Sandvol, E., Seber, D., Barazangi, M., Vidal, F., Alguacil, G., and Jabour, N., 2000, Propagation of regional seismic phases (Lg and Sn) and Pn velocity structure along the Africa-Iberia plate boundary zone: Tectonic implications: *Geophysical Journal International*, v. 142, p. 384–408.
- Chinn, D. S., Isacks, B. L., and Barazangi, M., 1980, High-frequency seismic wave propagation in western South America along the continental margin, in the Nazca plate and across the Altiplano: *Geophysical Journal of the Royal Astronomical Society*, v. 60, p. 209–244.
- Egorkin, A. V., and Pavlenkova, N. I., 1981, Studies of mantle structure of U.S.S.R. territories on long-range seismic profiles: *Physics of the Earth and Planetary Interiors*, v. 25, p. 12–26.
- Fuchs, K., Tittgemeyer, M., Ryberg, T., and Wenzel, F., 2002, Plate-wide  $S_p/P_n$  propagation and a schlieren waveguide in the uppermost mantle. in Cloetingh, S., and Ben-Avraham, Z., eds., From continental extension to collision: Africa-Europe interaction, the Dead Sea, and analogue natural laboratories: Katlenburg-Lindau, Germany, Copernicus GmbH, EGS—Stephan Mueller Special Publication Series, in press.
- Gettrust, J. F., and Frazer, L. N., 1981, A computer model study of the propagation of long-range  $P_n$  phase: *Geophysical Research Letters*, v. 8, p. 749–752.
- Gutenberg, B., 1954, Low-velocity layers in the earth's mantle: *Bulletin of the Geological Society of America*, v. 65, p. 337–348.
- Kadinsky-Cade, K., Barazangi, M., Oliver, J., and Isacks, B., 1981, Lateral variations of high frequency seismic wave propagation at regional distances across the Turkish and Iranian Plateaus: *Journal of Geophysical Research*, v. 86, p. 9377–9396.
- Kennett, B. L. N., 1989, On the nature of regional seismic phases—I. Phase representations for Pn, Pg, Sn, Lg: *Geophysical Journal*, v. 98, p. 447–456.
- Kennett, B. L. N., Engdahl, E. R., and Buland, R., 1995, Constraints on seismic velocities in the earth from traveltimes: *Geophysical Journal International*, v. 122, p. 108–124.

- Lehmann, I., 1964, On the velocity of P in the upper mantle: *Bulletin of the Seismological Society of America*, v. 54, p. 1097–1103.
- Linehan, D., 1935, Earthquakes in the West Indian region: EOS (Transactions of the American Geophysical Union), v. 21, p. 229–232.
- Mainprice, D., and Silver, P. G., 1993, Interpretation of SKS-waves using samples from the subcontinental lithosphere: *Physics of the Earth and Planetary Interiors*, v. 78, p. 257–280.
- Mallick, S., and Frazer, L. N., 1990,  $P_n/S_n$  synthetics for a variety of oceanic models and their implications for the structure of the oceanic lithosphere: *Geophysical Journal International*, v. 100, p. 235–253.
- Mechie, J., Egorkin, A. V., Fuchs, K., Ryberg, T., Solodilov, L., and Wenzel, F., 1993, P-wave mantle velocity structure beneath northern Eurasia from long-range recordings along the profile Quartz: *Physics of the Earth and Planetary Interiors*, v. 79, p. 269–286.
- Menke, W. H., and Chen, R., 1984, Numerical studies of the coda falloff rate of multiply-scattered waves in randomly layered media: *Bulletin of the Seismological Society of America*, v. 74, p. 1605–1621.
- Menke, W. H., and Richards, P., 1980, Crust-mantle whispering gallery phases: A deterministic model of teleseismic  $P_n$  wave propagation: *Journal of Geophysical Research*, v. 85, p. 5416–5422.
- , 1983, The horizontal propagation of P waves through scattering media: Analog model studies relevant to long-range  $P_n$  propagation: *Bulletin of the Seismological Society of America*, 73, 125–142.
- Mohorovicic, A., 1910, Das Beben vom 8.X.1909: *Jahrbuch des Meteorologischen Observatoriums in Zagreb (Agram) für das Jahr 1909, Band 9, Teil 4, Abschnitt 1*, p. 1–63.
- Molnar, P., and Oliver, J., 1969, Lateral variations of attenuation in the upper mantle and discontinuities in the lithosphere: *Journal of Geophysical Research*, v. 74, p. 2648–2682.
- Morozov, I. B., 2000, Comment on “High-frequency wave propagation in the uppermost mantle” by T. Ryberg and F. Wenzel: *Journal of Geophysical Research*, v. 106, p. 30,175–30,718.
- Mooney, W. D., and Brocher, T. M., 1987, Coincident seismic reflection/refraction studies of the continental lithosphere: A global review: *Reviews of Geophysics*, v. 25, p. 723–742.
- Ni, J. F., and Barazangi, M., 1983, High frequency seismic wave propagation beneath the Indian shield, Himalayan, Tibetan plateau and the surrounding regions: High uppermost mantle velocities and efficient  $S_n$  propagation beneath Tibet: *Geophysical Journal of the Royal Astronomical Society*, v. 72, p. 665–689.
- Nyblade, A. A., Vogtfjord, K. S., and Langston, C. A., 1996, P wave velocity of Proterozoic upper mantle beneath central and southern Asia: *Journal of Geophysical Research*, v. 101, B5, p. 11,159–11,171.
- Polet, J., and Kanamori, H., 2002, Anisotropy beneath California: Shear wave splitting measurements using a dense broadband array: *Geophysical Journal International*, v. 149, p. 313–327.
- Rapine, R. R., Ni, J. F., and Hearn, T. M., 1997, Regional wave propagation in China and its surrounding regions: *Bulletin of the Seismological Society of America*, v. 87, p. 1622–1636.
- Richards, P. G., and Menke, W. H., 1983, The apparent attenuation of a scattering medium: *Bulletin of the Seismological Society of America*, v. 73, p. 1005–1021.
- Rodgers, A. J., Ni, J. F., and Hearn T. M., 1997, Propagation characteristics of short-period  $S_n$  and  $L_g$  in the Middle East: *Bulletin of the Seismological Society of America*, v. 87, p. 396–413.
- Ryberg, T., Fuchs, K., Egorkin, A. V., and Solodilov, L., 1995, Observation of high-frequency teleseismic  $P_n$  on long-range QUARTZ profile across northern Eurasia: *Journal of Geophysical Research*, v. 100, p. 18,151–18,163.
- Ryberg, T., and Tittgemeyer, M., 2000, Finite difference modeling of seismic wave phenomena within the Earth’s upper mantle: HPCSE ‘2000, Lecture Notes on Computer Science and Engineering. Berlin, Germany and New York, NY, Springer.
- Ryberg, T., Tittgemeyer, M., and Wenzel, F., 2000a, Finite difference modeling of elastic wave propagation in the Earth’s uppermost mantle, in Krause, E., and Jäger, W., editors, HPCSE’99, Lecture Notes on Computer Science and Engineering. Berlin, Germany and New York, NY, Springer, p. 3–12.
- , 2000b, Finite difference modeling of P-wave scattering in the upper mantle: *Geophysical Journal International*, v.141, p.787–800.
- Ryberg, T., and Wenzel, F., 1999, High-frequency wave propagation in the uppermost mantle: *Journal of Geophysical Research*, v. 104, p.10,655–10,666.
- , 2002, Reply to Morozov (2000): *Journal of Geophysical Research*, in press.
- Sereno, T. J., and Orcutt, J. A., 1985, Synthesis of realistic oceanic  $P_n$  wave trains: *Journal of Geophysical Research*, v. 90, p. 12,755–12,776.
- , 1987, Synthetic  $P_n$  and  $S_n$  phases and the frequency dependence of Q of oceanic lithosphere: *Journal of Geophysical Research*, v. 92, p. 3541–3566.
- Sobolev, S. V., Zeyen, H., Granet, M., Achauer, U., Bauer, C., Werling, F., Altherr, R., and Fuchs, K., 1997, Upper mantle temperatures and lithosphere-asthenosphere system beneath the French Massif Central constrained by seismic, gravity, petrologic and thermal observations, in Fuchs, K., Altherr, R., Mueller, B., and Prodehl, C., eds., Stress and stress release in the lithosphere: *Tectonophysics*, v. 275, nos. 1-3, p. 143–164.

- Thybo, H., and Perchuc, E., 1997, The seismic 8° discontinuity and partial melting in continental mantle: *Science*, v. 275, p. 1626–1629.
- Tittgemeyer, M., 1999, Streuung elastischer Wellen im Erdmantel: Unpubl. Ph.D. thesis, Faculty of Physics, University of Karlsruhe, 131 p.
- Tittgemeyer, M., Ryberg, T., Wenzel, F., and Fuchs, K., 2002, Heterogeneities of the Earth's uppermost mantle, in Goff, J., and Holliger, K., eds., Small-scale crustal heterogeneities: Dordrecht, Netherlands, Kluwer Academic Publishers, in press
- Tittgemeyer, M., Wenzel, F., and Fuchs, K., 2000, On the Nature of  $P_n$ : *Journal of Geophysical Research*, v. 105, p. 16,173–16,180.
- Tittgemeyer, M., Wenzel, F., Fuchs, K., and Ryberg, T., 1996, Wave propagation in a multiple scattering upper mantle—observations and modeling: *Geophysical Journal International*, v. 127, p. 492–502.
- Tittgemeyer, M., Wenzel, F., Ryberg, T., and Fuchs, K., 1999, Scales of heterogeneities in the continental crust and upper mantle: *Pure and Applied Geophysics*, v. 156, p. 29–52.
- Turcotte, D., and Schubert, G., 1982: *Geodynamics—Application of continuum physics to geological problems*: New York, John Wiley & Sons, 450 p.
- Walker, D., 1977, High frequency  $P_n$  and  $S_n$  phases recorded in the western Pacific: *Journal of Geophysical Research*, v. 82, p. 3850–3360.
- , 1981, High frequency  $P_n$  and  $S_n$  velocities—some comparisons for the western, central, and south Pacific: *Geophysical Research Letters*, v. 9, p. 207–209.
- Wenzel, F., Fuchs, K., Enderle, U., and Tittgemeyer, M., 1997, Elastic properties of crust and upper mantle—a new view: *Proceedings of the 30th International Geological Congress*, v. 4, Structure of the lithosphere and deep processes, p. 31–43.